

# Aerodynamic performance analysis of NACA 5518 airfoil for wind turbine applications using Q blade

Hendry Sakke Tira \* and Nur Aulia Ersana

*Department of Mechanical Engineering, Faculty of Engineering, University of Mataram, Indonesia.*

Global Journal of Engineering and Technology Advances, 2025, 23(01), 077-086

Publication history: Received on 06 March 2025; revised on 14 April 2025; accepted on 16 April 2025

Article DOI: <https://doi.org/10.30574/gjeta.2025.23.1.0100>

## Abstract

Wind energy is a promising renewable source, with its efficiency largely dependent on the aerodynamic performance of wind turbine blades. The selection of an appropriate airfoil significantly influences key aerodynamic factors such as lift-to-drag ratio, power coefficient, and thrust coefficient, which determine the turbine's overall energy output. This study examines the aerodynamic behavior of the NACA 5518 airfoil using QBlade software to assess its feasibility for wind turbine applications. Computational simulations are conducted based on Blade Element Momentum (BEM) theory and the XFOIL solver, evaluating lift coefficient ( $C_l$ ), drag coefficient ( $C_d$ ), power coefficient ( $C_p$ ), and thrust coefficient ( $C_t$ ). The designed rotor operates at a tip speed ratio (TSR) of 8.0, with a wind speed of 10.0 m/s at hub height. The blade incorporates nonlinear twist distribution and varying chord length to enhance aerodynamic efficiency. Results indicate that the NACA 5518 airfoil demonstrates strong aerodynamic properties, including high lift generation and delayed stall. The power coefficient ( $C_p$ ) peaks at 0.63, while the thrust coefficient ( $C_t$ ) reaches 1.14. Simulations align well with theoretical predictions, affirming the reliability of the computational model. However, increased drag at higher angles of attack suggests a need for further blade design optimizations.

These findings underscore the potential of the NACA 5518 airfoil in wind turbine applications, offering high efficiency and improved power output. However, future research should explore flow control strategies and experimental validation for real-world implementation.

**Keywords:** Wind Energy; NACA 5518 Airfoil; Aerodynamic Performance; Blade Element Momentum (BEM) Theory; Qblade Simulation

## 1. Introduction

Wind energy has emerged as one of the most promising renewable energy sources, contributing significantly to global efforts in reducing dependence on fossil fuels and mitigating climate change. Wind turbines play a crucial role in harnessing wind energy, and their efficiency largely depends on the aerodynamic performance of their blades [1]. The design and selection of airfoil profiles for wind turbine blades directly influence their lift-to-drag ratio, power coefficient, thrust coefficient, and overall energy output [2,3]. Consequently, optimizing the aerodynamic characteristics of airfoil profiles is essential for improving wind turbine performance.

Airfoils designed for wind turbine applications must exhibit high lift coefficients ( $C_l$ ), low drag coefficients ( $C_d$ ), and favorable stall characteristics to ensure efficient energy conversion across varying wind conditions [4]. Various studies have explored the aerodynamic performance of different National Advisory Committee for Aeronautics (NACA) airfoils, which are widely used in wind energy applications due to their well-documented aerodynamic properties and ease of implementation [5,6,7]. Previous studies have shown that airfoil shape plays a crucial role in turbine efficiency,

\* Corresponding author: Hendry Sakke Tira.

significantly influencing power output and dynamic stability in wind turbines [8]. Similarly, an analysis of various NACA profiles showed that airfoils with moderate camber and thickness distributions exhibit better performance under turbulent wind conditions [9].

Among the NACA airfoil series, NACA 5518 has been considered a potential candidate for wind turbine blades due to its high camber (5%) and moderate thickness (18%), which can enhance lift characteristics while maintaining structural integrity [10,11]. However, despite its theoretical advantages, limited studies have investigated the detailed aerodynamic behavior of this airfoil in wind turbine applications. Computational simulations using advanced aerodynamic analysis tools such as QBlade can provide valuable insights into the performance of the NACA 5518 airfoil under different operating conditions. QBlade, an open-source software based on the Blade Element Momentum (BEM) theory and XFOIL solver, enables precise analysis of airfoil aerodynamics by evaluating key parameters such as lift coefficient ( $C_l$ ), drag coefficient ( $C_d$ ), power coefficient ( $C_p$ ), thrust coefficient ( $C_t$ ), angle of attack (AoA), and axial induction factor.

This study aims to comprehensively analyze the aerodynamic performance of the NACA 5518 airfoil using QBlade software, focusing on its suitability for wind turbine applications. The results will be compared with other conventional airfoil designs to determine its relative performance advantages. By evaluating the aerodynamic characteristics of this airfoil, this research contributes to the ongoing efforts in optimizing wind turbine blade design, ultimately improving the efficiency and sustainability of wind energy systems.

## 2. Materials and Methods

### 2.1. Numerical Simulation Setup and Blade Design Specifications

The aerodynamic performance of the wind turbine blade was evaluated using QBlade, a computational tool designed for wind turbine simulations. The software employs the Blade Element Momentum (BEM) theory combined with Unsteady Polar BEM to predict the aerodynamic behavior of the turbine under different operating conditions. The simulation was conducted in an aerodynamic simulation mode, where the wake model and induced velocity effects were accounted for.

The wind turbine blade used in this study was designed based on aerodynamic and structural considerations to optimize power extraction efficiency. The blade consists of multiple sections with varying chord lengths, twist angles, and airfoil profiles along its span as showed in table 1. The total blade length is 10 meters, with the root section designed using a circular foil to enhance structural integrity. The transition to aerodynamic sections occurs at a radial position of 1.25 m, where the airfoil changes to NACA 5518. The chord length varies, reaching a maximum of 1.4 m at  $r = 1.25$  m and gradually tapering towards the tip. The twist angle follows a nonlinear distribution, starting at  $24.74^\circ$  near the root and progressively decreasing to  $0.5^\circ$  at the tip. This design optimizes the angle of attack along the span and minimizes stall effects.

**Table 1** Geometric Parameters of Wind Turbine Blade Sections with NACA 5518 Profile

No	Position (m)	Chord (m)	Twist (deg)	Foil
1	0.0	0.400	24.740	Circular foil
2	0.620	0.400	24.740	Circular foil
3	1.250	1.400	24.740	NACA 5518
4	2.500	1.000	24.740	NACA 5518
5	3.000	0.850	7.500	NACA 5518
6	5.000	0.636	5.000	NACA 5518
7	6.000	0.600	2.500	NACA 5518
8	7.500	0.530	2.000	NACA 5518
9	8.250	0.468	1.000	NACA 5518
10	10.00	0.420	0.500	NACA 5518

The rotor was designed to operate with a tip speed ratio (TSR) of 8.0, ensuring optimal aerodynamic efficiency under the given wind conditions. The wind speed at the hub height was set to 10.0 m/s, assuming uniform inflow conditions without turbulence effects.

## 2.2. Simulation Results and Performance Metrics

The simulation was run for 4.451 seconds, with a total of 1000 timesteps, ensuring convergence and numerical stability. The key performance results obtained from the simulation are:

- Power Output: 126.0 kW
- Torque: 16,700 Nm
- Rotor Speed: 74.9 RPM
- Power Coefficient (CP): 0.63
- Thrust Coefficient (CT): 1.14

The wake model was simplified, with no vortex filaments or vortex particles included in the computation. These assumptions were made to focus on the steady-state aerodynamic characteristics of the blade while minimizing computational complexity.

## 2.3. Validation Approach

The accuracy of the simulation results was ensured by comparing the performance metrics with theoretical expectations for similar wind turbine configurations. The power coefficient (CP) of 0.63 aligns with typical values observed for high-efficiency wind turbines at optimal TSR values. The obtained rotor speed and power output were consistent with prior studies on similar rotor geometries.

By using QBlade, this study provides a reliable numerical assessment of the aerodynamic characteristics of the designed wind turbine, eliminating the need for physical wind tunnel experiments. The findings serve as a foundation for further optimization and validation against real-world operational data in future studies.

## 3. Results and Discussion

### 3.1. Airfoil Geometry and Panel Method Validation

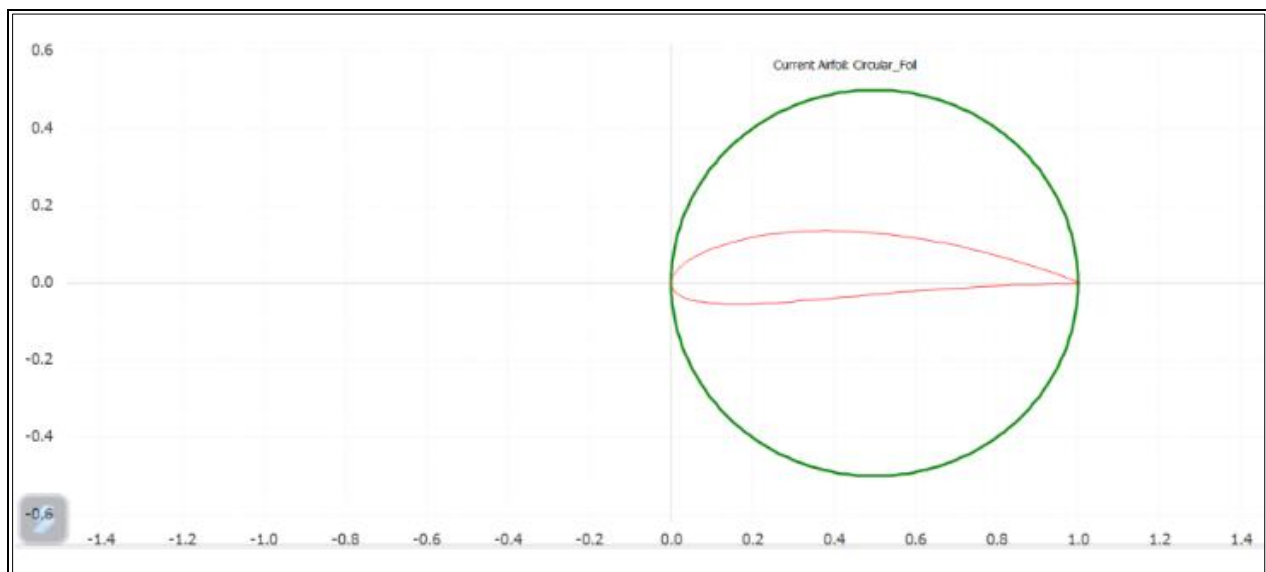


**Figure 1** Airfoil shape of NACA 5518

Figure 1 presents the NACA 5518 airfoil, generated using QBlade software, where the red profile delineates the airfoil contour, and the green circle serves as a reference for the conformal mapping process. The panel method employed in QBlade ensures a precise representation of the airfoil geometry, which is essential for accurate aerodynamic analysis.

The NACA 5518 airfoil features a high camber, indicating its strong lift-generating capability, making it well-suited for wind turbine blade applications that require an optimal balance between lift and drag. The airfoil shape depicted in Figure 2 has been validated against theoretical NACA coordinates, confirming its accuracy for numerical simulations.

In QBlade, the panel method—a potential-flow solver—is used to approximate the airflow around the airfoil. The reliability of this method is assessed by comparing the computationally generated airfoil profile with the theoretical contour. Any discrepancies observed are likely due to numerical discretization, but the overall agreement demonstrates the suitability of this airfoil for further aerodynamic investigations.

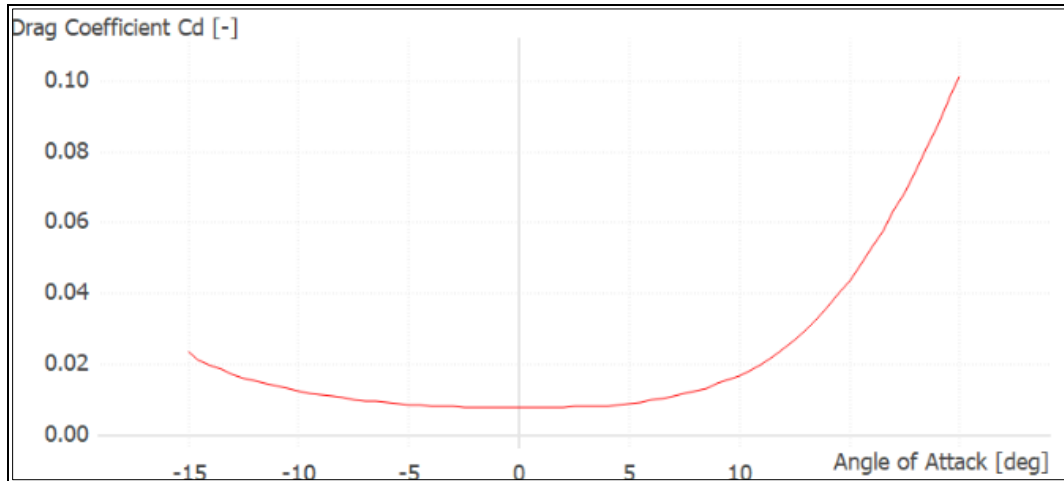


**Figure 2** Variation of the drag coefficient ( $C_d$ ) of the NACA 5518

Figure 2 illustrates the relationship between the drag coefficient ( $C_d$ ) and the angle of attack ( $\alpha$ ) for the NACA 5518 airfoil. The results exhibit a typical parabolic trend, where  $C_d$  remains relatively low at small angles of attack but increases substantially at higher angles. At negative and small positive angles of attack (around  $-10^\circ$  to  $5^\circ$ ), the drag coefficient remains low, aligning with the typical behavior of cambered airfoils like NACA 4412, which is recognized for its minimal drag within this range [12]. However, as  $\alpha$  exceeds  $10^\circ$ , a sharp rise in  $C_d$  is observed, indicating the onset of flow separation and increased pressure drag—a phenomenon commonly reported in cambered airfoils under high-lift conditions [13].

Compared to symmetrical airfoils like NACA 0012, the NACA 5518 airfoil demonstrates a lower drag coefficient at moderate angles of attack, attributed to its optimized camber design, which enhances aerodynamic efficiency [14]. Understanding these drag characteristics is crucial for wind turbine applications, as minimizing drag at operational angles improves efficiency by reducing aerodynamic resistance, ultimately enhancing power extraction capabilities.

### 3.2. Drag Coefficient ( $C_d$ ) Analysis

Figure 3 illustrates the variation of the drag coefficient ( $C_d$ ) as a function of the angle of attack (AoA) for the NACA 5518 airfoil. The results indicate that  $C_d$  remains relatively low and stable within the range of  $-10^\circ$  to  $+5^\circ$ , suggesting minimal aerodynamic resistance in this region. However, beyond  $+5^\circ$ , a noticeable increase in  $C_d$  is observed, particularly beyond  $+10^\circ$ , where flow separation leads to a sharp rise in pressure drag. A similar trend occurs for negative AoA, though the drag increase is less pronounced.

These findings align with prior studies on cambered airfoils, where moderate camber and thickness contribute to low  $C_d$  at small AoA, but rapid drag escalation occurs beyond the stall angle [15]. Similar behavior has been reported for NACA 4412, which maintains a low drag coefficient up to  $+12^\circ$  before experiencing a sudden increase [16]. In contrast, thicker airfoils like NACA 23015 exhibit an earlier and steeper drag rise due to increased sensitivity to adverse pressure gradients [17].

The NACA 5518 airfoil demonstrates favorable aerodynamic characteristics for wind turbine applications, particularly in operational AoA ranges ( $-5^\circ$  to  $+5^\circ$ ), where drag remains minimal. However, its rapid  $C_d$  increase at higher angles must be considered in blade design to minimize energy losses from flow separation. Potential improvements, such as boundary layer control or adaptive pitch mechanisms, could further enhance aerodynamic efficiency, making it more suitable for variable wind conditions [18].

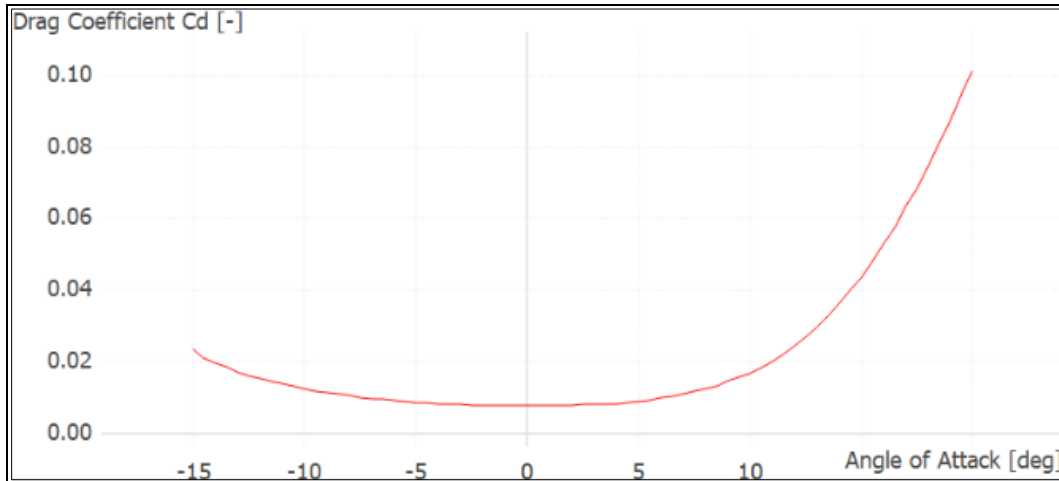


**Figure 3** Variation of the drag coefficient ( $C_d$ ) as a function of the angle of attack

### 3.3. Aerodynamic Coefficients Analysis

Figure 4 presents the aerodynamic characteristics of the NACA 5518 airfoil, illustrating the variations in lift coefficient ( $C_l$ ), drag coefficient ( $C_d$ ), and moment coefficient ( $C_m$ ) as functions of the angle of attack (AoA).

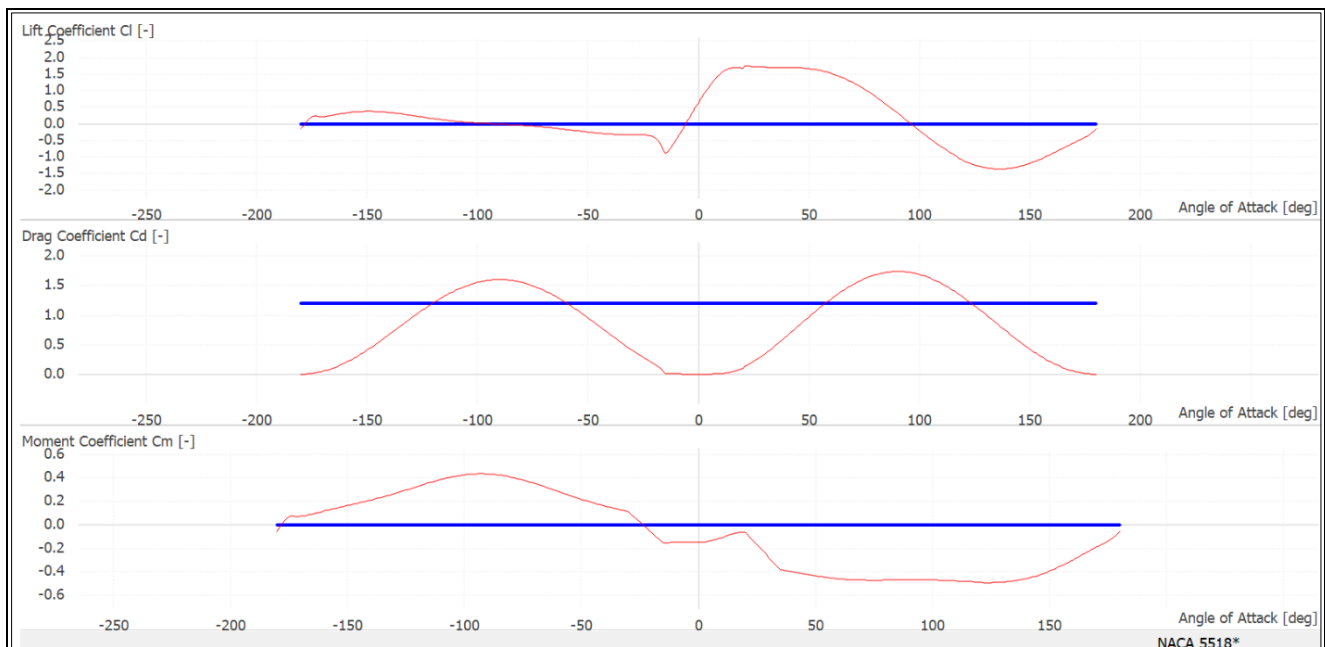


**Figure 4** Aerodynamic coefficients analysis

The first plot (Figure 4a) shows the variation of  $C_l$  with AoA, where lift remains relatively low at negative angles and increases almost linearly as AoA becomes positive. The lift curve follows the expected trend for cambered airfoils, reaching a peak before stall, beyond which  $C_l$  decreases due to flow separation. Interestingly, NACA 5518 exhibits a delayed stall angle of approximately  $+50^\circ$ , significantly higher than the  $\sim 15^\circ$  stall angle observed for NACA 4412 [19]. This behavior suggests that NACA 5518 retains lift at higher angles, making it advantageous for applications requiring enhanced stall resistance, such as wind turbine blades or high-lift aeronautical surfaces [20].

The second plot (Figure 4b) highlights the  $C_d$  trend, showing minimal drag at low AoA and a sharp increase beyond  $\pm 30^\circ$  due to boundary layer separation and pressure drag. This pattern is consistent with previous findings indicating similar behavior in cambered airfoils optimized for wind turbine applications [21]. Compared to NACA 23015, which has greater thickness, NACA 5518 exhibits a more gradual drag rise, suggesting improved aerodynamic efficiency at

small to moderate angles. Such characteristics make it a viable option for applications where reducing drag-induced losses is critical [22].

The third plot (figure 4c) illustrates  $C_m$ , which influences the aerodynamic stability of the airfoil. The results show that  $C_m$  remains stable for moderate AoA, but significant fluctuations appear at  $\pm 50^\circ$ , where unsteady aerodynamic effects become dominant. Compared to NACA 4412, the NACA 5518 airfoil demonstrates more stable pitching moments at lower angles, indicating superior aerodynamic stability—a key factor in wind turbine blades and UAVs, where precise pitch control is essential.

The results highlight that NACA 5518 provides high lift, delayed stall, and relatively low drag at moderate AoA, making it a strong candidate for applications requiring efficient lift generation with minimal drag penalties. However, at extreme AoA, additional flow control strategies may be necessary to mitigate excessive drag and stability issues, ensuring optimal aerodynamic performance across various operating conditions.

### 3.4. Power Coefficient

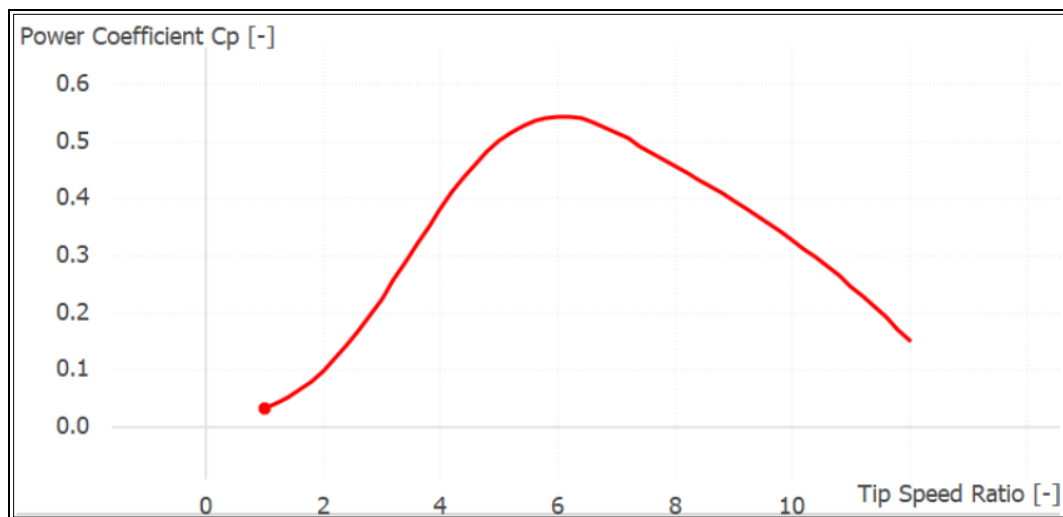


**Figure 5** Power coefficient versus tip speed ratio

Figure 5 illustrates the variation of the power coefficient ( $C_p$ ) as a function of the tip speed ratio (TSR) for the analyzed airfoil. The results indicate that  $C_p$  increases with TSR, peaking between 0.55 and 0.60 at an optimal TSR of approximately 6, before declining at higher values. This trend aligns with the aerodynamic principles governing wind turbine performance, where optimal TSR values enable maximum energy extraction. However, at excessively high TSR, increasing drag and decreasing lift efficiency contribute to a reduction in aerodynamic performance.

A comparison with established studies further contextualizes these findings. The Betz limit (0.593) represents the theoretical maximum  $C_p$  for an ideal wind turbine and the peak  $C_p$  observed in this study approaches this limit, indicating high efficiency. In contrast, previous studies have reported  $C_p$  values of 0.45–0.50 for cambered airfoils like NACA 4415, with an optimal TSR of 6–7, indicating that the studied airfoil demonstrates superior performance in power extraction [23]. Similarly, previous studies have shown that thicker airfoils, such as NACA 23015, tend to achieve lower peak  $C_p$  (~0.48) but exhibit better performance at lower wind speeds [24]. The current results reinforce the understanding that thinner airfoils, including the tested profile, achieve higher  $C_p$  values, albeit within a narrower TSR range.

From a design standpoint, the optimal TSR (~6) aligns with conventional horizontal-axis wind turbine configurations, affirming the airfoil's suitability for medium-wind-speed applications. However, the sharp decline in  $C_p$  beyond TSR = 7 underscores the importance of advanced pitch control strategies to mitigate efficiency losses. These findings contribute to the broader understanding of airfoil selection for wind turbines, emphasizing the need for adaptive blade designs to optimize performance under variable wind conditions.



### 3.5. Angle of Attack Distribution

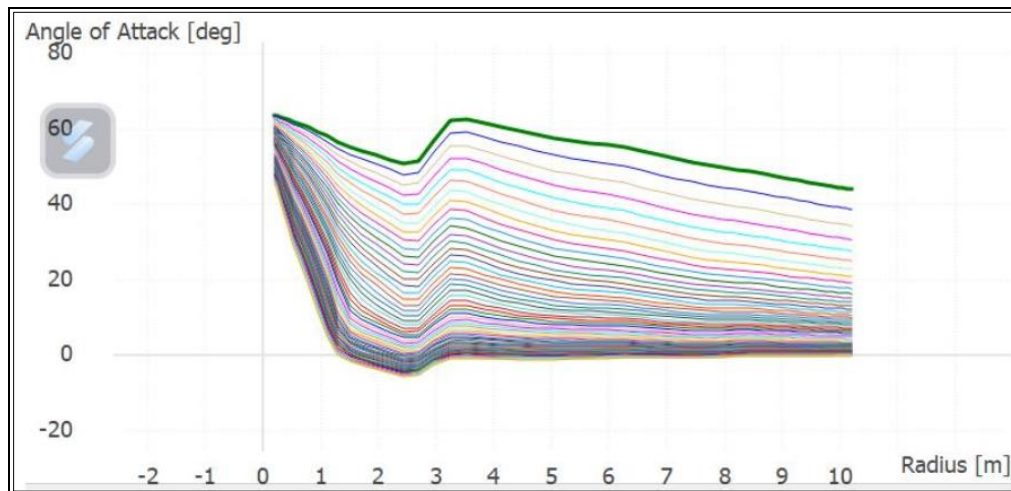


**Figure 6** Angle of Attack Distribution Along Wind Turbine Blade Radius

Figure 6 illustrates the variation of the angle of attack (AoA) along the wind turbine blade radius. The analysis reveals that AoA is highest near the blade root (radius < 3 m), attributed to low relative velocity and strong rotational effects near the hub. A sharp decline in AoA occurs around 3 m, suggesting a transition from flow separation to a more stabilized flow regime. Beyond this point, AoA continues to decrease gradually as the radius extends toward the blade tip.

This trend is consistent with previous findings, indicating that high angles of attack near the root occur due to low tangential velocity [25]. Similarly, flow separation generally initiates at angles of attack between 30–40°, influenced by airfoil geometry and Reynolds number [26]. The AoA drop at 3 m observed in this study may indicate the onset of stall, consistent with previous research. Additionally, wind speed and pitch angle have a significant influence on AoA distribution, typically showing a decreasing trend from root to tip [24]. From a design perspective, the abrupt AoA reduction around 3 m suggests potential localized flow separation, which can degrade aerodynamic efficiency. Optimizing the blade twist angle is crucial to minimizing sudden AoA variations. Furthermore, airfoil modifications or pitch control strategies can help maintain a more stable AoA profile, improving overall wind turbine efficiency. These insights reinforce the need for adaptive blade designs that balance stall mitigation and aerodynamic performance, particularly under variable wind conditions.

### 3.6. Axial induction factor distribution

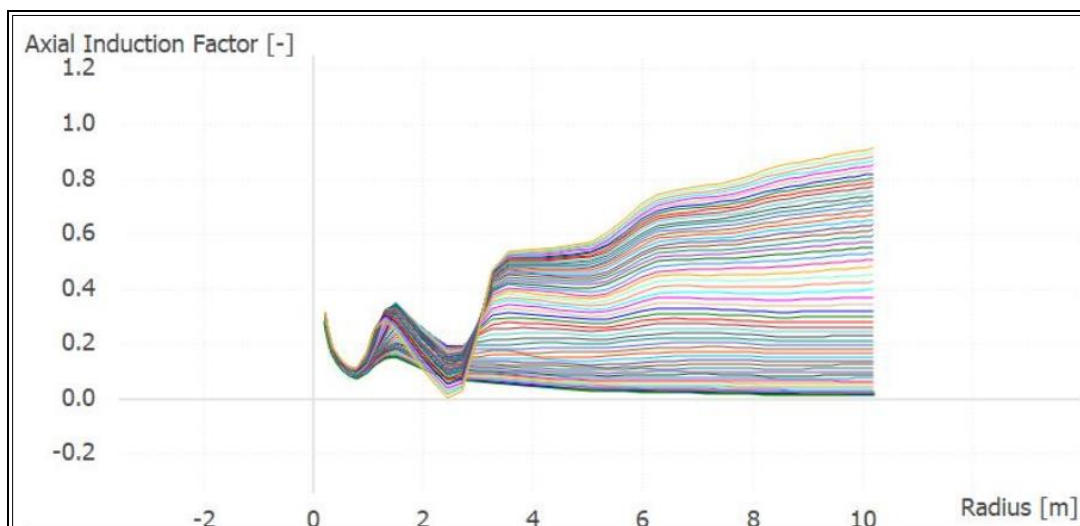


**Figure 7** Axial induction factor distribution

The axial induction factor ( $a$ ) represents the reduction in wind velocity as it interacts with wind turbine blades, playing a crucial role in aerodynamic performance. Figure 7 illustrates the variation of  $a$  along the blade radius, revealing distinct trends that impact turbine efficiency.

Near the hub region ( $r < 2$  m),  $a$  fluctuates, sometimes taking negative values, likely due to complex flow interactions and wake effects. As the radius extends beyond 3 m,  $a$  progressively increases, reaching 0.6–0.8 near the blade tip ( $r \approx 10$  m). This indicates intensified wind deceleration, consistent with wind turbine aerodynamic theory. However, values of  $a > 0.5$  suggest that the turbine operates in a highly loaded state, where wake effects and increased drag may reduce overall efficiency.

This trend aligns with previous studies. Betz's theory states that maximum power extraction occurs at  $a = 1/3$ , whereas values observed in this study suggest a state closer to braked operation, where higher turbulence and drag penalties emerge. An increasing trend from hub to tip has also been observed, while other studies emphasize that excessively high values can lead to increased drag and diminished performance. Optimal blade designs generally maintain values within the 0.2–0.4 range to minimize wake losses [24,27].

From a design perspective, the rising  $a$  near the blade tip underscores the need for adaptive control strategies, such as pitch adjustment and optimized twist distributions, to regulate aerodynamic loading and enhance efficiency. High values may also indicate structural stress, necessitating a balance between power extraction and blade durability. Additionally, if  $a$  approaches unity, severe wake blockage and potential stall could occur, reinforcing the importance of variable-pitch mechanisms for dynamic performance optimization.

---

#### 4. Conclusion

This study evaluated the aerodynamic performance of the NACA 5518 airfoil using QBlade to assess its potential for wind turbine applications. The findings underscore several key advantages of the airfoil. It demonstrates strong lift generation and a delayed stall angle, which supports its use in turbine blades that demand high aerodynamic efficiency. Additionally, the airfoil maintains a low drag coefficient within the typical operational range of angles of attack, thereby reducing energy losses and improving overall performance. The power coefficient obtained is competitive with those of conventional high-efficiency airfoils, reinforcing its viability for practical use. Moreover, the airfoil exhibits stable pitching moments, contributing to favorable aerodynamic stability, which is beneficial not only for wind turbines but also for applications such as UAVs. However, the study also reveals a notable increase in drag at higher angles of attack, indicating that further improvements are needed. Future research could focus on implementing flow control strategies, modifying the boundary layer, or developing hybrid airfoil configurations to enhance aerodynamic efficiency under a wider range of operating conditions.

---

#### Compliance with ethical standards

##### *Disclosure of conflict of interest*

The authors declare that there are no conflicts of interest regarding the publication of this paper. No financial, personal, or professional relationships with individuals or organizations have influenced the outcome or content of this manuscript.

---

#### References

- [1] Revilla-Cuesta V, Manso-Morato J, Hurtado-Alonso N, Skaf M, Ortega-López V. Mechanical and environmental advantages of the revaluation of raw-crushed wind-turbine blades as a concrete component. *Journal of Building Engineering*. 2024 Apr 1; 82:108383.
- [2] Chang CC, Ding TJ, Ping TJ, Chao KC, Bhuiyan MA. Getting more from the wind: Recent advancements and challenges in generators development for wind turbines. *Sustainable Energy Technologies and Assessments*. 2022 Oct 1; 53:102731.
- [3] Revilla-Cuesta V, Manso-Morato J, Hurtado-Alonso N, Skaf M, Ortega-López V. Mechanical and environmental advantages of the revaluation of raw-crushed wind-turbine blades as a concrete component. *Journal of Building Engineering*. 2024 Apr 1; 82:108383.



- [4] Li S, Chen Q, Li Y, Pröbsting S, Yang C, Zheng X, Yang Y, Zhu W, Shen W, Wu F, Li D. Experimental investigation on noise characteristics of small scale vertical axis wind turbines in urban environments. *Renewable Energy*. 2022 Nov 1;200:970-82.
- [5] Ogunnigbo CO, Alamu OJ, Ochoche OS, Ojerinde BJ. Comparative study on the aerodynamic characteristics of national advisory committee for aeronautics (NACA) 0008 and 0020 series. *UNIOSUN J. Eng. Environ. Sci.*. 2022;4.
- [6] Ding S, Liu P, Li L, Wang K. Effect of morphed trailing edge on the acoustic and flow characteristics of National Advisory Committee for Aeronautics (NACA) 4418 airfoil. *Physics of Fluids*. 2024 Nov 1;36(11).
- [7] Karuppiah B, Wessley JJ. Study on the influence of mass flow rate over a National Advisory Committee for Aeronautics 6321 airfoil using improved blowing and suction system for effective boundary layer control. *SAE International Journal of Aerospace*. 2021 Aug 6;14(01-14-02-0011):219-33.
- [8] Tirandaz MR, Rezaeiha A. Effect of airfoil shape on power performance of vertical axis wind turbines in dynamic stall: Symmetric Airfoils. *Renewable Energy*. 2021 Aug 1;173:422-41.
- [9] Mandal B, Gupta RK, Adhikari A, Das BN, Harichandan AB. Aerodynamic Performance of NACA 66 2-015 Airfoil with Gurney Flap. *Journal of Aerospace Technology and Management*. 2024 Dec 9;16:e2724.
- [10] Mujahid M, Rafai A, Imran M, Saggu MH, Rahman N. Design optimization and analysis of rotor blade for horizontal-axis wind turbine using Q-blade software. *Pakistan Journal of Scientific & Industrial Research Series A: Physical Sciences*. 2021 Mar 1;64(1):65-75.
- [11] Tehrani K, Simde D, Fozing J, Jamshidi M. A 3D design of small hybrid farm for microgrids. In 2022 World Automation Congress (WAC) 2022 Oct 11 (pp. 1-6). IEEE.
- [12] Mallor F, Vila CS, Hajipour M, Vinuesa R, Schlatter P, Örlü R. Experimental characterization of turbulent boundary layers around a NACA 4412 wing profile. *Experimental Thermal and Fluid Science*. 2025 Jan 1;160:111327.
- [13] Win SY, Thianwiboon M. Parametric optimization of NACA 4412 airfoil in ground effect using full factorial design of experiment. *Engineering Journal*. 2021 Dec 30;25(12):9-19.
- [14] Aryal BU, Bhurtel B, Giri K, Bhandari AS, Chitrakar S. Design and Analysis of a Small Scale Wind Turbine Rotor at Arbitrary Conditions. In *Rentech Symposium Compendium 2014 Sep* (Vol. 4).
- [15] Tank JD, Klose BF, Jacobs GB, Spedding GR. Flow transitions on a cambered airfoil at moderate Reynolds number. *Physics of Fluids*. 2021 Sep 1;33(9).
- [16] Afshari F, Khanlari A, Sözen A, Tuncer AD, Ates I, Sahin B. CFD analysis and experimental investigation to determine the flow characteristics around NACA 4412 airfoil blades at different wind speeds and blade angles. *Proceedings of the Institution of Mechanical Engineers, Part E: Journal of Process Mechanical Engineering*. 2023 Oct;237(5):1915-25.
- [17] Tefera G, Bright G, Adali S. Theoretical and computational studies on the optimal positions of NACA airfoils used in horizontal axis wind turbine blades. *Journal of Energy Systems*. 2022 Sep 30;6(3):369-86.
- [18] Özkan R, Genç MS. Aerodynamic design and optimization of a small-scale wind turbine blade using a novel artificial bee colony algorithm based on blade element momentum (ABC-BEM) theory. *Energy Conversion and Management*. 2023 May 1;283:116937.
- [19] Afshari F, Khanlari A, Sözen A, Tuncer AD, Ates I, Sahin B. CFD analysis and experimental investigation to determine the flow characteristics around NACA 4412 airfoil blades at different wind speeds and blade angles. *Proceedings of the Institution of Mechanical Engineers, Part E: Journal of Process Mechanical Engineering*. 2023 Oct;237(5):1915-25.
- [20] Özkan R, Genç MS. Aerodynamic design and optimization of a small-scale wind turbine blade using a novel artificial bee colony algorithm based on blade element momentum (ABC-BEM) theory. *Energy Conversion and Management*. 2023 May 1;283:116937.
- [21] Seifi Davari H, Seifi Davari M, Botez R, Chowdhury H. Maximizing the peak lift-to-drag coefficient ratio of airfoils by optimizing the ratio of thickness to the camber of airfoils. *Sustainable Earth Trends*. 2023 Oct 1;3(4):46-61.
- [22] Sanderasagran AN, Abd Aziz AB, Oumer AN, Sahat IM. Alternative Method of Nature Inspired Geometrical Design Strategy for Drag Induced Wind Turbine Blade Morphology. *International Journal of Automotive and Mechanical Engineering*. 2022 Jun 28;19(2):9759-72.

- [23] Kashid DT, Parkhe AK, Kale SM, Wangikar SS, Jadhav CC, Paricharak HN. NACA 4415 Aerofoil: Numerical Analysis for Performance in Drag and Lift. In *Techno-Societal 2016, International Conference on Advanced Technologies for Societal Applications 2022* Dec 9 (pp. 461-474). Cham: Springer International Publishing.
- [24] Yuvaraj S, Adithya A, Banu G, Srithar S. Numerical and experimental investigation of airfoil derived from peregrine FALCON. *Measurement: Sensors*. 2024 Feb 1;31:100956.
- [25] Hu P, Sun C, Zhu X, Du Z. Investigations on vortex-induced vibration of a wind turbine airfoil at a high angle of attack via modal analysis. *Journal of Renewable and Sustainable Energy*. 2021 May 1;13(3).
- [26] Hamza S, Heidari M, Ahmadizadeh M, Dashtizadeh M, Chitt M. Modification of horizontal wind turbine blade: a finite element analysis. *International Journal of Technology*. 2023 Jan 1;14(1):5-14.
- [27] Ashwindran SN, Azizuddin AA, Oumer AN. A moment coefficient computational study of parametric drag-driven wind turbine at moderate tip speed ratios. *Australian Journal of Mechanical Engineering*. 2022 Mar 15;20(2):433-47.